Arabian Journal of Geosciences (2021) 14: 2086
https://doi.org/10.1007/s12517-021-08430-3

REVIEW PAPER

New insights into the dynamic characteristics of alluvial media under the earthquake prone area: a case study for the Çanakkale city settlement (NW of Turkey)

Aydın Büyüksaraç[1] · Tolga Bekler[2] · Alper Demirci[2] · Onur Eyisüren[3]

Received: 7 June 2021 / Accepted: 9 September 2021 / Published online: 30 September 2021

Abstract

Çanakkale is a settlement located in the northwest of Turkey with relatively low strength soils under high seismic hazard. The depth of the bedrock was calculated based on microtremor measurements as the resonance frequency was variable, and a correlation was obtained by performing regression analysis based on the exponential variation trend curve. At the same time, resonance frequency values obtained from Çanakkale soils were recalculated as variables with 30 depth-resonance frequency correlations obtained before. The variation of the regression coefficients with the depths of the basin was examined. Especially, it has been observed that *a-coefficient* can be grouped with four different depths based on value ranges.

Keywords Alluvial thickness · Ambient noise · Çanakkale · Microtremor · Resonance frequency

Introduction

Loose soils are the basis of many geotechnical problems due to their low density, high compressibility, and low strength. These properties make them potentially collapsible, causing large foundation settlements even under low loads (Delgado et al. 2000a). Thus, determination of the weathered uppermost layer thickness consisting of incompetent, loose units is one of the basic inputs for regional seismic hazard analyses. A large seismic impedance contrast between the unconsolidated sediments and the bedrock may make it possible to determine the cover layer thickness. Determination of the engineering bedrock depth is essential to reveal the influence of dynamic soil conditions and building damage potential during an earthquake. For this purpose, a direct relationship between resonance frequency and sediment thickness can be established using the findings of deep targeted geophysical surveys and/or observations of a sufficient number of boreholes which contain information about depth down to the bedrock in the regional scale (Gosar and Lenart 2010). Soil behavior can be determined in a simple, low-cost way without much scrutinizing the geological structure of the underground with the Horizontal-to-Vertical-Spectral-Ratio (HVSR) (Nakamura 1989) method. Afterwards, the microtremor survey method has been used as a powerful tool of predictive approach to map the thickness of sediments (Ibs-von Seht and Wohlenberg 1999).

In the northwestern part of the Biga Peninsula, the alluvial structure in the Çanakkale Basin, which lies along the seacoast, was investigated using the ambient noise measurements via HVSR technique and MASW method.

The studied basin is located at the western end of the North Anatolian Fault Zone (NAFZ) in a region subject to high seismic hazard (Fig. 1). Çanakkale and its surroundings were affected by many earthquakes with M>6.0 in the historical and instrumental period.

Especially, in the South Marmara Region, Saros Bay earthquakes on the northern branch of the NAFZ and active earthquakes in Yenice and Edremit segments on the southern branch of the NAFZ have been threaten Çanakkale and its vicinity. Destructive earthquakes in historical period, documented by Ambraseys and Finkel (1995), are shown in Fig. 2a.

Responsible Editor: Longjun Dong

✉ Aydın Büyüksaraç
absarac@comu.edu.tr

[1] Çan Vocational School, Çanakkale Onsekiz Mart University, TR-17400 Çan/Çanakkale, Turkey

[2] Department of Geophysical Engineering, Çanakkale Onsekiz Mart University, TR-17000 Çanakkale, Turkey

[3] School of Graduate Studies, Çanakkale Onsekiz Mart University, TR-17100 Çanakkale, Turkey

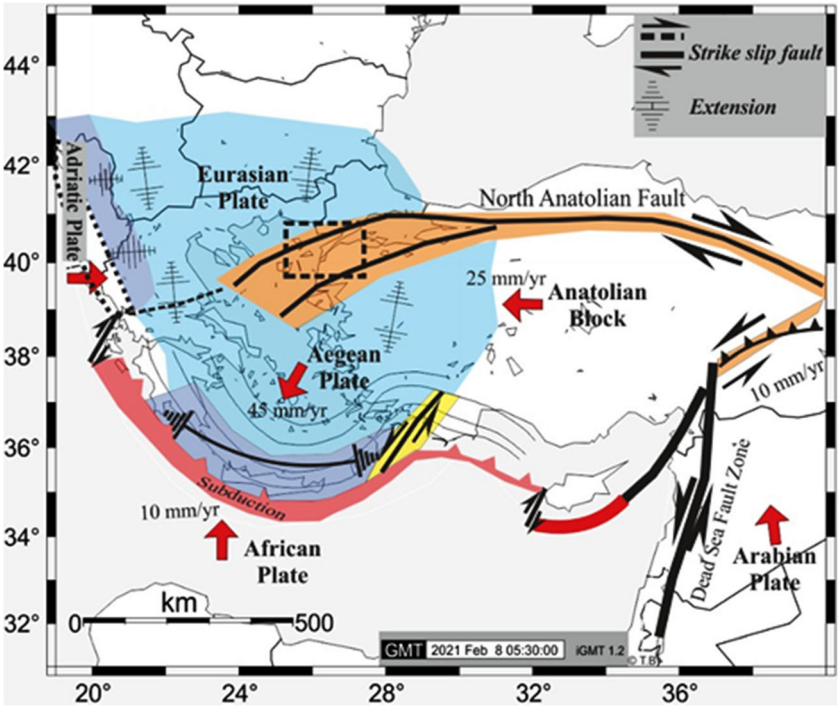

Fig. 1 Simplified tectonic frame of Anatolian block and surrounding area. Red short arrows represent plate motion directions, thick and black arrows represent generalized directions of fault zones, and dashed and bidirectional arrows represent extension zones

As in the historical period, devastating earthquakes occurred in this important and seismically active zone in the instrumental period. Murefte-Sarkoy earthquake (Ms = 7.3) is one of the largest earthquakes recorded in western Turkey, on the Ganos fault segment at the northern edge of the NAFZ which occurred in 1912 and was recorded in a large area as well as the Balkans countries. The magnitude of the largest aftershock that occurred approximately one month after the main shock was measured as Ms=6.3. The other remarkable earthquake on this branch occurred at Gökçeada offshore in the Aegean Sea (Mw = 6.8) in 2014 and caused partial damage in Çanakkale.

There are four major earthquakes in the lower arm in the instrumental period. The Ms=7.0 near Edremit in 1919, Mw = 6.8 on the Sarıköy Fault in 1944, Ms = 7.2 known as the Yenice-Gönen earthquake in 1953, and M = 7.2 of the Edremit Bay in 1981 are characteristic earthquakes (Fig. 2b). The earthquakes that recently occurred in Ayvacık also took place on this branch. Numerous studies have been published on the seismicity of Northwest Anatolia (Kürçer et al. 2008; Özden et al. 2018; Ganas et al. 2019; Bekler and Demirci 2018; Gorgun and Albora 2017; Gorgun et al. 2020).

Middle-Upper Miocene aged terrestrial and marine sedimentary rock units deposited in the Çanakkale Basin crop out along the eastern edge of the Çanakkale Strait (Dardanelles). These sediments unconformably overlie Paleozoic metamorphics, Permian-Triassic ophiolites, and Eocene volcanic rocks between Çanakkale and Troy (Atabey et al. 2004). Shear wave velocity (Vs) and compression wave velocity (Vp) values were determined by making MASW measurements to obtain shallow soil properties as well as microtremor measurements in the ground surveys conducted in Çanakkale central settlement (Bekler et al. 2019). However, the pattern and seismic source characteristics used for these measurements are not sufficient to define the seismic model of the basin, reaching an average depth of 10 m.

The aim of this study is to determine the looser layer thickness and the depth of seismic bedrock in Çanakkale Basin, which is thought to have very thick deposits. The fact that the Çanakkale Basin structure is quite deep causes uncertainty in urban development, especially stability problems such as low bearing capacity, liquefaction, and low lateral resistance to shear coefficients.

This study will be a guide to reveal the deep structure of the Çanakkale Basin, which is thought to contain very thick sedimentary units, and if possible, the loose layer thickness, i.e., the bedrock/seismic basement depth. Various methods are used to determine the depth of the bedrock, in other words the thickness of the cover layer or sedimentary units on the bedrock. However, the necessary support for these works that require a significant budget and time cannot always be provided easily. In this case, it is planned to find a new solution to solve the problem of a data set based on existing information in the study area. Some researchers who have previously worked on this subject have developed correlations based on field-specific experimental approaches to calculate the deep structure, especially the depth of bedrock, using nonlinear regression relationships from in situ geophysical data

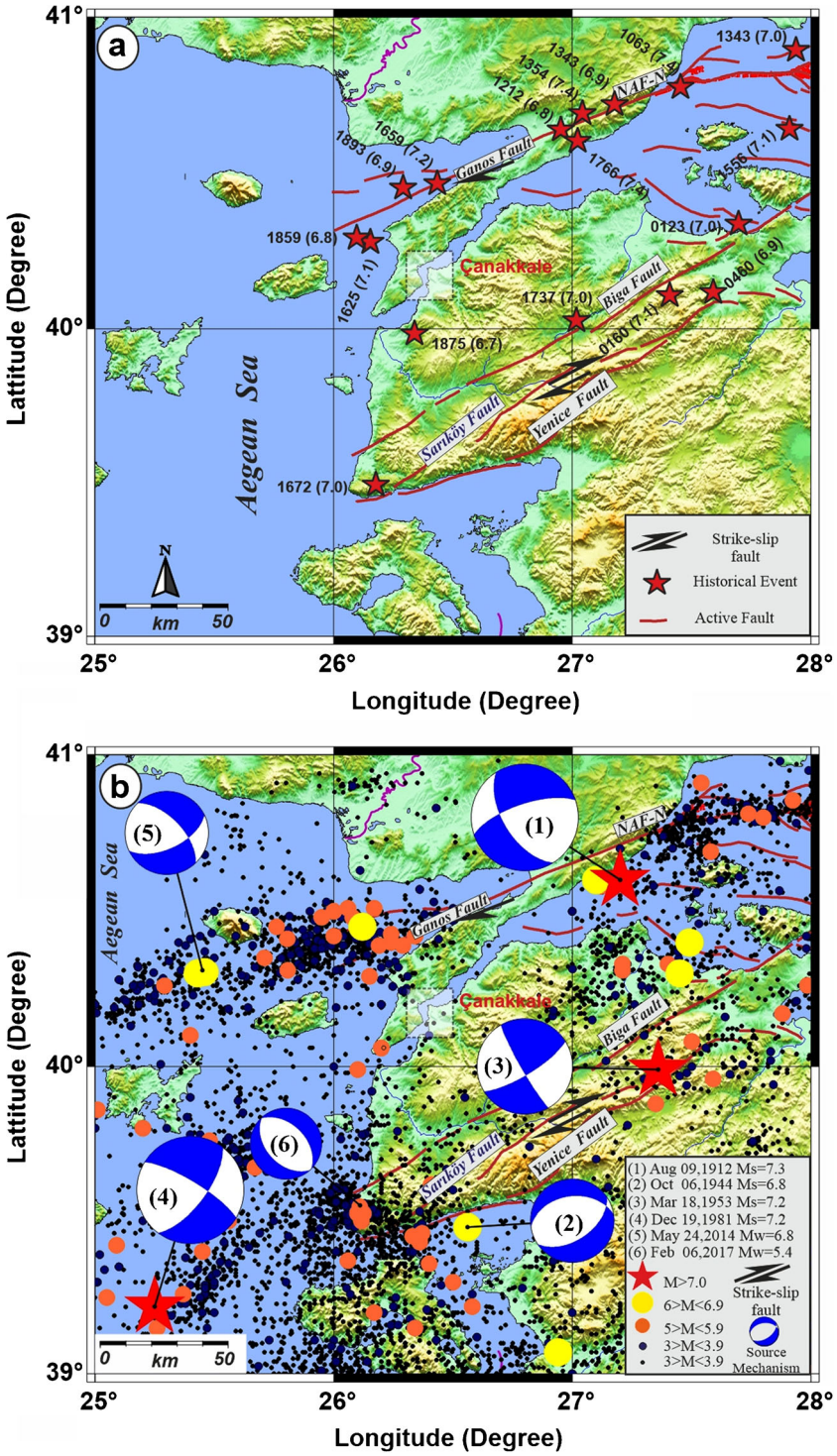

Fig. 2 (**a**) The historical earthquakes occurred in Çanakkale and its vicinity are shown with red stars on the simplified tectonic map. (**b**) Earthquakes that occurred in Çanakkale and its vicinity between 1900 and 2020 ($M \geq 3.0$). Fault mechanism solutions for medium and large earthquakes ((*1*,*3*, Görgun et al, 2020), (*2*, Altınok et al., 2012), (*6*, Bekler and Demirci 2018), and (*5*, Kalafat et al., 2014))

(Thabet 2019). Most of these studies aimed to obtain bedrock depth from resonance frequency values. Yamanaka et al. (1994) and Field (1996) generally examined the process of defining the depth-resonance frequency (*h-fr*) relationship and determining the coefficients of curvature parameters *a* and *b* (Eq. 1).

$$h = a f r^{-b} \tag{1}$$

where *h* is depth, *fr* is resonance frequency, and *a* and *b* are the regression coefficients. The obtained curves essentially define an exponential function. When 30 studies that they were performed in different zones in the world so far are examined, it is observed that the *b-coefficient* generally takes values between 1 and 1.5 in the developed relations and does not show much deviation (Fig. 3). When the graph is

examined, deviations out of range were observed in 5 studies. In contrast, *a-coefficient* is more variable. In this case, the idea that the value of *a-coefficient* can be a characteristic parameter for each region comes to the fore (Gosar and Lenart 2010). At the same time, Thabet (2019) focused on the results of researchers who have conducted similar studies to date and formed the depth-frequency (*h-f*) experimental relationship and determined that the upper layer-bedrock interface significantly affects the frequency-depth relationships.

Geological setting

The study area is represented by the Çanakkale Group, whose Miocene-Holocene geology is essentially compatible with a distinct angular unconformity on paleotectonic basement rocks older than itself. Çanakkale Group is of Middle-Upper Miocene age and sits on units older than itself with an angular discordance. Miocene rocks older than this and are the continuation of Oligocene volcanic/volcaniclastic units below this discordance are considered as bedrock rocks in this study. Çanakkale Group, which is located on metamorphic and magmatic basement units with an angle unconformity, consists of alluvial fan sediments. Çanakkale Group consists of Gazhanedere, Kirazlı, Çamraktepe, and Alçıtepe members with different lithological assemblages, sedimentary features, and sedimentation environments. These members are laterally and vertically transitive with each other. The unit, called the Gazhanedere Formation, is a very loosely heterogeneous unit. Due to this characteristic and location, its outcrops have mostly undergone deformation at different degrees. For this reason, it has gained a different structural character compared to the units it is in contact with, and its relationship with the overlying units has been interpreted as "discordant" in previous studies. Kirazlı Formation also passes to Çamrakdere Formation with lateral and vertical transition towards the top. Çamrakdere Formation consists of mudstone, marl, siltstone, sandstone, calcarenite, and in places fine conglomerate. The lithology is marls and mudstones, and it shows itself in typical beige, gray, and greenish gray-bluish gray colors. Other lithological units are mostly found in lenticular geometries or interlayers in marl and mudstones. The unit consisting of marl and mudstone, which is essentially impermeable and changes in volume in contact with water, and the porous loosely attached clastic rock intermediate levels and lenses in them cause significant stability problems in periods where climatic conditions allow. Çamrakdere Formation gradually passes to the Alçıtepe Formation towards the uppermost surface. Alçıtepe Formation consists of fossil limestone and siltstone and marls alternating with it. The Alçıtepe Formation, which forms the top of the Miocene units outcropping on the slopes on both sides of the Çanakkale Strait (Dardanelles), forms building platforms at approximately 150 m altitude on the Gelibolu Peninsula and 350 m on the Biga Peninsula. Alçıtepe member is composed of algae diffuse limestone, oolitic limestone deposited in shallows, beach conglomerate, and coarse sandstone. The Upper Miocene Çanakkale Group is overlain by Pleistocene marine terraces and Pleistocene-current alluvial deposits (Fig. 4) (Atabey et al. 2004; Yiğitbaş 2015).

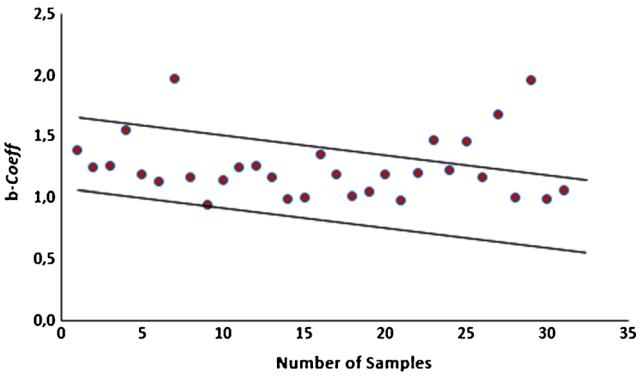

Fig. 3 The interval of change of the *b-coefficient* in 30 relations examined in this article

Method

Microtremor and MASW measurements were performed at 110 points in an area covering Çanakkale city settlement (Fig. 5). Alçıtepe Formation containing claystones and sandy limestones is in the B-Zone to the north of the study area. The A1-Zone located in the north of this area and the center, east, and south (A2-Zone) of the area are formed from the Quaternary aged alluvial stream sediments of the old bed of Sarıçay passing through Çanakkale city center. The C-Zone located in the southeast of the study area constitutes the Gazhanedere Formation with mudstone supported conglomerates and loosely cemented. The liquefaction intensity index of the entire area, except for the B-Zone in the north and the C-Zone in the southeast of the study area, was determined to be high and very high (Bekler et al. 2019; Tunusluoğlu and Karaca 2018).

At these locations, three-component microtremors were recorded for an average of 25–35 min with a sampling frequency of 100 Hz. The data collected with the GURALP CMG-6TD broad-band seismometer were converted to digital data with the help of an integrated 24-bit digitizer and then recorded on the internal disk in GCF format. Time series including microtremors in three-components in a wide frequency range from 0.033 to 50 Hz were recorded instantaneously with the seismometer. To obtain the H/V curve, the GEOPSY open-source software package is an efficient signal processing tool implemented by SESAME Project (Wathelet et al. 2020). This software uses information such as recording time, data length, sampling interval, number of components to calculate

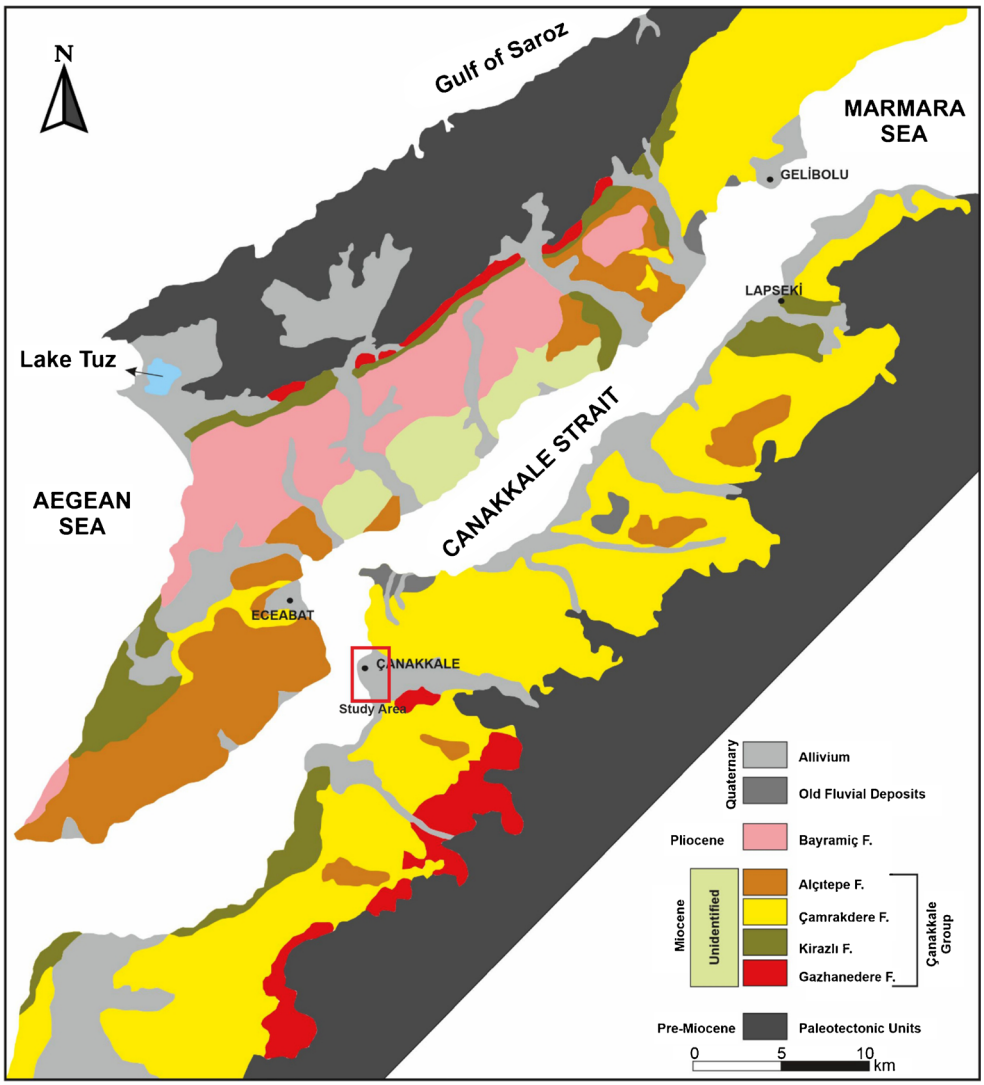

Fig. 4 Geological map of Biga and Gelibolu peninsulas near Çanakkale Strait (Amended from Yiğitbaş 2015 and Atabey et al. 2004). Red rectangular exhibits study area

resonant frequency (*fr*), and amplification (*Ao*) parameters from spectral amplitude ratios of horizontal and vertical component just as implemented in Nakamura (1989) approach. The entire recorded time series is divided into several sub-windows to select data subsets which do not include the influence of industrial and other cultural noises as much as possible by the GEOPSY software. The further process is to calculate the Fourier transformed amplitude spectra of each component and obtain the H/V spectrum. The standard procedure of HVSR uses geometric mean of the two horizontal spectra for each sub-window. Calculated ratios from large number of recording time windows are averaged in the final process. At this stage, the bandwidth coefficient of 40 was selected and achieved smoothing with the Konno and Omachi (1998) filter. H/V graphics representing different zones of the study area are shown in Fig. 6.

Average shear velocity (*Vs*30) was obtained from seismic profiles at the same location as each microtremor measurement point (Fig. 5). Profile directions have been chosen to best reflect the working area considering the field conditions. Although the spacing of the geophones with a natural frequency of 4.5 Hz varies according to the location of the measurement point, it was generally 2 m and the off-set distance was chosen 6, 8, and 10 m considering the formation of the surface wave. Thus, it was aimed to investigate depth of up to 30 m. Record length and sampling interval was 1 sec and 0.125 msec. The fundamental mode dispersion curves were determined by taking the seismic sections obtained by measurements into the frequency-wave number domain (Fig. 7). After frequency filtering and spectral trace corrections, the theoretical dispersion curve was formed by making an iterative inverse solution. The inversion procedure consists of trying *Vs* models, computing the theoretical dispersion curve from the model, comparing with the experimental one, and evaluating the misfit, proposing a new *Vs* model with some criterion such as the misfit value and number of iterations. *Vs* velocities and depths were calculated for each layer as a result by the inversion of the obtained curve. Many theoretical

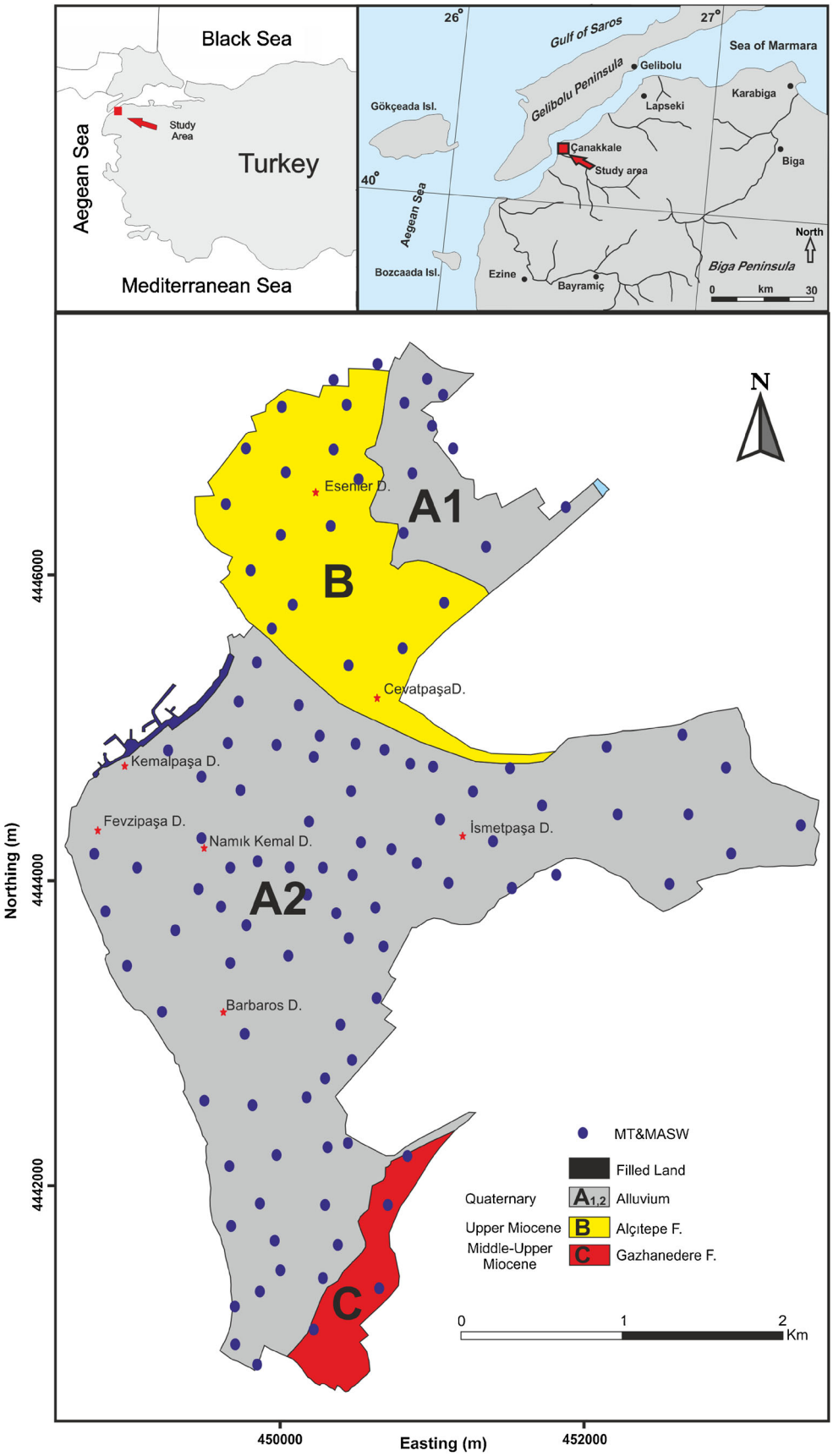

Fig. 5 Distribution of MASW and microtremor measurement points on ground units in Çanakkale city center

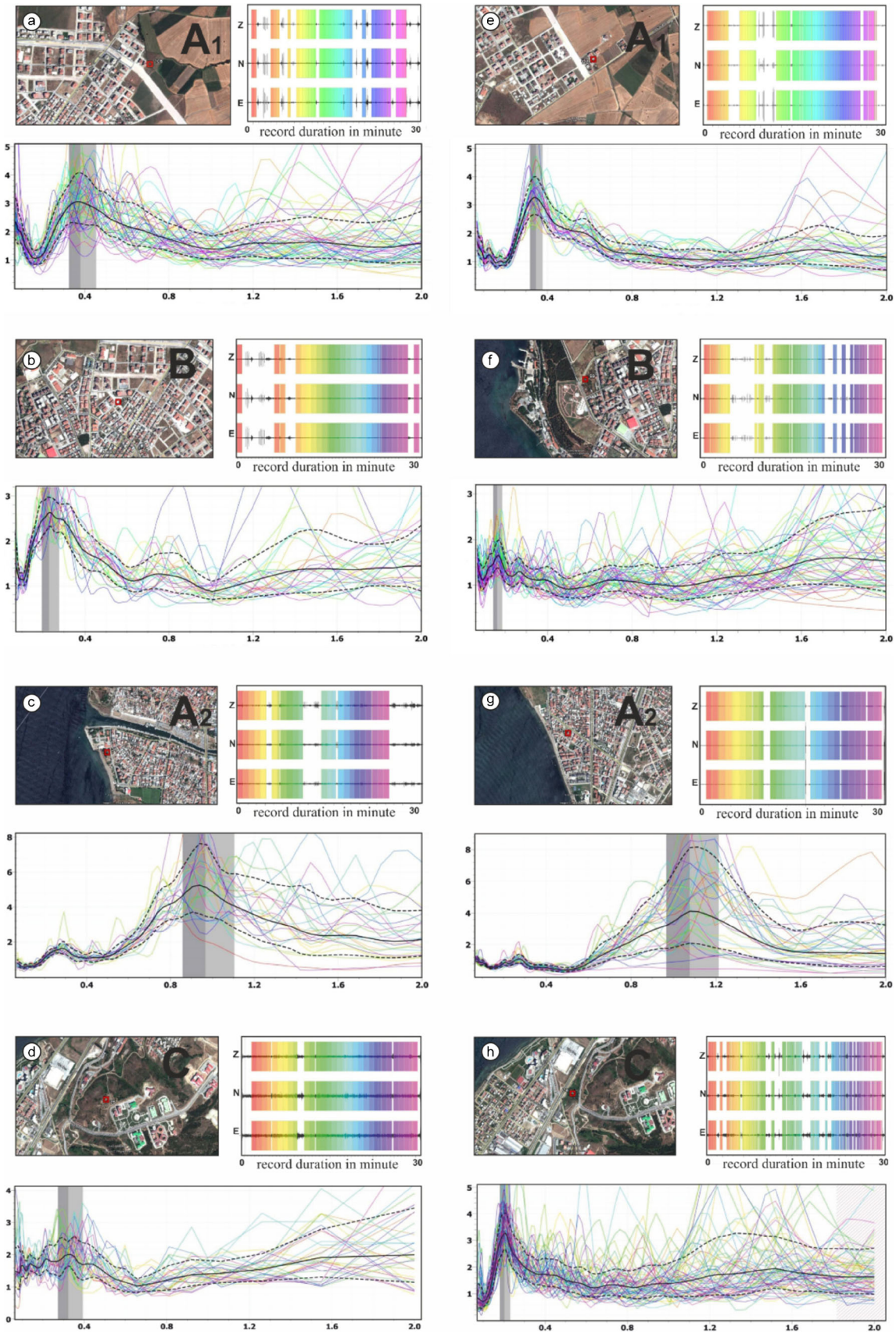

Fig. 6 Seismic noise measurement records of selected time windows with low gained amplitudes and H/V spectral ratios at different site conditions based on surface geology

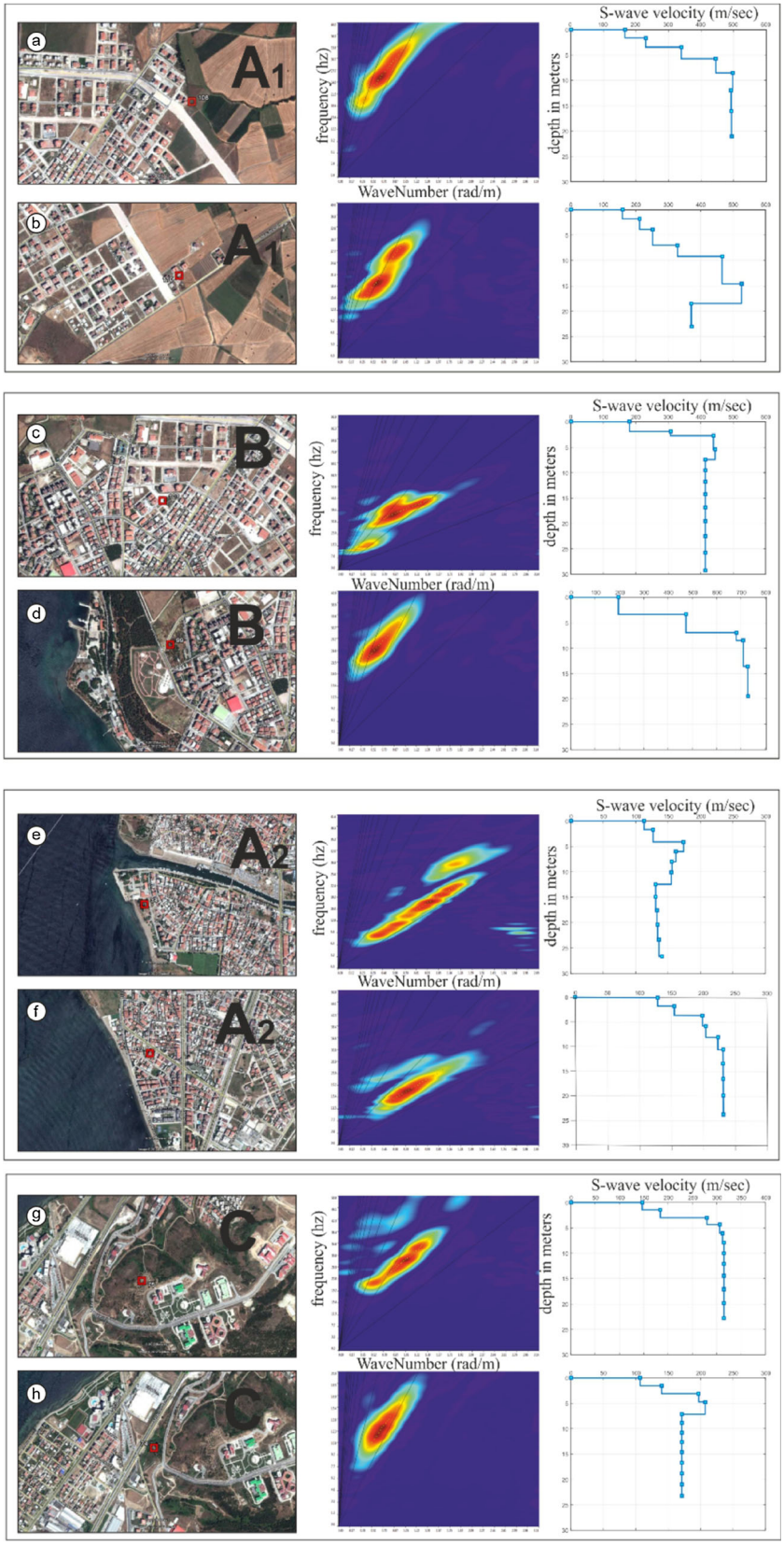

Fig. 7 Frequency-wave number (f–k) spectrums and S-wave velocity variations modeled from linear array MASW measurements at different site conditions influenced by different surface geology. The fundamental modes are visible in red to yellow colored scale

dispersion curves are computed, and probably even the last one will be different from the experimental one.

Some experimental researches (Nakamura 1989; Lermo and Chavez-Garcia1994 have shown that some information

can be obtained from a single station ambient noise recording using the HVSR technique. If there is a homogeneous sedimentary cover and a sufficiently high mechanical contrast with the underlying materials, the resonance frequency approximately corresponds to $fr = Vs/4h$ at the HVSR, where Vs is the shear velocity in the loose layer and h is its thickness. Kuo et al. (2016) suggested 600 msec^{-1} as the Vs velocity of the engineering bedrock. The seismic basement velocity value suggested by Nakamura (2008) is 760 msec^{-1}. Rayleigh waves, whose particle motion is elliptical and whose motion is in the opposite direction to the propagation direction, propagate in a semi-infinite homogeneous elastic medium (Aki 1965). Rayleigh waves must be spread in a layered environment in order to show dispersion. Ellipticity is not fixed, and particle motion changes from reverse elliptical movement to forward elliptical movement depending on the contrast between the bedrock and the ground. Ellipticity can be determined by the H/V spectral ratio between the peak in the fundamental resonance frequency and the first minimum in the high frequency (Fah et al. 2001). Therefore, 1-dimensional S-wave velocity structure of the ground can be revealed by using the shape of the H/V spectral ratio. The inverse solution of the ellipticity curves of Rayleigh waves is made using the Dinver software from the Geopsy package (www.geopsy.org) based on the neighborhood algorithm. Before the inverse solution, the number of loose layers on the bedrock, the range of thickness (hmin and hmax), densities (min and max), body wave velocity intervals (Vp and Vs), Poisson's ratio, and parameters are determined and used as input data in the software. During the inverse solution, only the ellipticity curves of Rayleigh waves are not enough to correlate depth and velocity values with each other. Therefore, such an inverse solution works in combination with the values obtained from the MASW analysis of the superficial Vs values for example. Calculations were made using the Rayleigh Elliptical method in order to determine the bedrock depths in the study area. Seismic bedrock depth was calculated at 50 points that could exceed 760 msec^{-1} velocities. A regression relation is established between the fr values that fulfill this condition and the corresponding depth (h) values as in Eq. (1).

This situation reveals the conditions in which the loose soil properties are considerable. Accordingly, the empirical correlation (2) was calculated by exponential regression which enables to obtain the bedrock depth easily for Çanakkale soils as below.

$$h = 86.176\left(fr^{-1.063}\right) \quad (2)$$

List of similar studies earlier in the world is given in Table 1. According to these studies, bedrock depths can be examined in four different groups. Accordingly, basin thicknesses reaching 1000 m and deeper are defined as *very deep*, those reaching a depth of about 500 m as *deep*, those reaching over 100 m as *medium deep*, and those below 100 m as *shallow* basin depths. Also, the depths grouped in Table 1 are expressed in different colors.

The regression curve showing the relationship established can be seen in Fig. 8. The scatter plot of resonance frequencies and calculated depths denotes that there is a significant clustering especially at low frequencies. Low-frequency environments often describe lose ground conditions. Such soils are also frequently encountered in basins. In this case, it should be expected to obtain scattered dominant vibration periods in environments where there is loose and shallow groundwater level in the basins.

Considering the soil conditions of corresponding studies, reported empirical functions of basins which have similar soil characteristics to Çanakkale Basin were compared with the function obtained from the current study.

The resonance frequency values obtained in the study area were recalculated with the equations obtained from areas with similar soil properties such as Cape Cod, Massachusetts (USA) (Fairchild et al. 2013), Ottawa (Canada) (Molnar et al. 2018), and Antakya (South Turkey) (Büyüksaraç et al. 2021). The results indicate that the equations can be used in many similar studies, depending on the resonance frequency and regression coefficients reflecting the soil properties and the depth range of the bedrock suitable (Fig. 9).

Results and discussion

It is important to determine the seismic hazard, which describes the magnitude of strong ground motion that an earthquake can cause, which is closely related to the damage potential. In addition, earthquake ground motion is closely related to the focal mechanism. The focal mechanism is an important feature of the seismic source, which has a major impact on the propagation of seismic waves (Ma et al. 2019). Even though the distance to the source is mostly the same, the dynamic conditions vary greatly in different directions (Ma et al. 2018, 2019. Therefore, it is necessary to understand the effects of the focal mechanism on the induced ground motions in the evaluation of seismic hazards. Ground motion is controlled by the combined effects of azimuth, source focus mechanism, distance, and source size and decreases linearly only in some specific propagation directions under certain focal mechanism (Ma et al. 2019). There is great uncertainty and variability associated with the spatial and temporal formation of seismicity. Focal mechanisms vary with stress field and geological conditions. PGV is considered the most representative parameter in determining dynamic loads. Defining the ground conditions up to the bedrock, especially in areas with high earthquake risk, is essential in order to accurately predict the consequences of earthquake ground motion. The depth to the

Table 1 Studies that developed a correlation between bedrock depth and resonance frequency. Coloring was made according to depth changes. Accordingly, the dark gray color is very deep, the gray color is deep, the light gray color is medium deep, and the white color is shallow bedrock depths

Code	Place	Reference	Equation	Site Type	Depth of Basin (m)
1	Western Lower Rhine Embayment (Germany)	Ibs-von Seht and Wohlenberg (1999)	$h=96(f_r^{-1.388})$	Soft Sediment	15–1600
2	Segura River Valley (Southeastern Spain)	Delgado et al. (2000a)	$h=55,11(f_r^{-1.256})$	Soft Sediment	4 to 44
3	Bajo Segura Basin (Southeastern Spain)	Delgado et al. (2000b)	$h=55,64(f_r^{-1.268})$	Soft Sediment	46
4	Cologne Area (Germany)	Parolai et al. (2002)	$h=108*(f_r^{-1.551})$	Sediment	20–1000
5	Lower Rhine Embayment (Germany)	Hinzen et al. (2004)	$h=137(f_r^{-1,19})$	Soft Sediment	70–1250
6	Zafarraya Basin (Spain)	García-Jerez et al. (2006)	$h=194,6(f_r^{-1,14})$	Clay and alluvial silt	11-125
7	Bam Area (Iran)	Motamed et al. (2007)	$h=135,2(f_r^{-1,979})$	Alluvial deposit	3-80
8	Florence Basin (Italy)	D'Amico et al. (2008)	$h=140(f_r^{-1,172})$	fluvio-lacustrine sediments	9-115
9	Bangalore region (India)	Dinesh et al. (2010)	$h=58.30(f_r^{-0.952})$	Rock Formation	3.5-26
10	Southern Coast of Istanbul (Turkey)	Birgören et al. (2009)	$h=150,99(f_r^{-1,153})$	Alluvium	20–449
11	Ljubljana Moor Basin (Slovenia)	Gosar and Lenart (2010)	$h=105,53(f_r^{-1,25})$	Quaternary lacustrine and fluvial sediments	0-200
12	Izmit Bay Area (Turkey)	Özalaybey et al. (2011)	$h=141(f_r^{1,27})$		20–1100
13	Western Sydney (Australia)	Harutoonian et al. (2013)	$h=73(f_r^{-1,17})$	Quaternary Alluvium	1.2–13.3
14	Cape Cod, Massachusetts (USA)	Fairchild et al. (2013)	$h=90,53(f_r^{-1})$	Unconsolidated sedments	118–460
15	L'Aquila, central (Italy)	Del Monaco et al. (2013)	$h=53,461(f_r^{-1,01})$	Soft Soil	3–<20
16	Eskisehir Basin (Turkey)	Tün et al. (2016)	$h=136(f_r^{-1,357})$	Quaternary Sediment	0–500
17	Ottowa (Canada)	Molnar et al. (2018)	$h=64.98(f_r^{-1.198})$	Soft glaciomarine, Soft Sediment	24,5-91
18	Pearl River Delta (China)	Liang et al. (2018)	$h=55(f_r^{-1.02})$	Sediment	8-40
19	Singapore	Moon et al. (2019)	$h=92,5(f_r^{-1.06})$	Alluvial deposit	28-36
20	Japan	Thabet (2019)	$h=117,13(f_r^{-1,197})$	Sediment	2–1500
21	Hatay (Turkey)	Büyüksaraç et al. (2021)	$h=101(f_r^{-0,988})$	Sedimantery	20-80
22	Katmandu an intermontane basin of Himalaya (Nepal)	Paudyal et al. (2013)	$h=146,01fr^{-1,2079}$	sedimantery	166-347
23	Narmada valley (Western India)	Sukumaran et al. (2011)	$h=102,1\ fr^{-1,47}$	Quaternary sediments	4-539 averagely 114
24	Islamabad (Pakistan)	Khan and Khan (2016)	$h = 134.06\ fr^{-1.23}$	Quaternary Deposits	2-141
25	Shillong City of Northeast India	Biswas et al. 2015	$h=160,94\ fr\ -^{1,459}$	Sediment	10-200
26	Indo-Gangetic Plain (India)	Anbazhagan et al. (2019)	$h=234,45\ fr^{-0,69}$ $h=137.88\ fr^{-1,174}$	alluvium deposit	102-1012
27	Upper Silesian Coal Basin Sosnowiec, Bytom and Chorzow (Poland)	Mendecki et al. (2014)	$h=59,626\ fr^{-1,68}$	Sediment	15-35
28	Qom Basin (Iran)	Maghami et al. 2021	$h=96,17\ fr^{-1,01}$	Quaternary Alluvium	80-100
29	Kachchh, Western India (India)	Sant et al. (2017)	$h =110,18fr^{-1.97}$	Quaternary sediment	35-115
30	Ljubljana Moor Basin (Central Slovenia)	Rupar and Gosar (2020)	$h=202,97\ fr^{-1.139}$	Unconsolidated sediments	110
31	Çanakkale Basin (Turkey)	*This Study*	$h = 86,176fr^{-1,063}$	Aluvial deposit	4-100

bedrock can be calculated with the help of empirical Eq. (1) in areas with basin-type characteristics such as alluvium or sedimentary structures on the bedrock. The *a-coefficient*, which is the main identifier in this equation, can vary over a wide range because it is affected by different soil conditions. The resonant frequency values obtained from Çanakkale soils were used as variable in the equations obtained from 30 different geographic locations, and the variation of the obtained graphics was observed. The 30 researches were divided into groups according to the depth of the studied basin, and the compatibility of

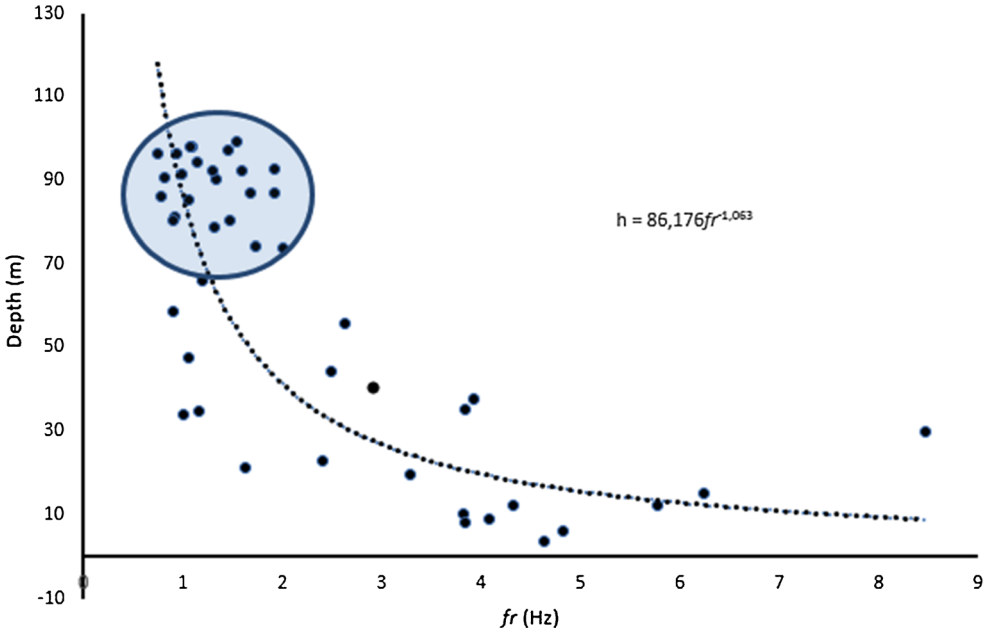

Fig. 8 Characteristic depth-resonance frequency correlation and variation for Çanakkale city

the *a-coefficient* variation with those in the corresponding group was investigated. Accordingly, the basins are divided into four different depth models as very deep, deep, medium deep, and shallow. Naturally, groupings within 30 samples do not consist of an equal number of samples. Depth of basins that can reach 1000 m and deeper are very deep, and examples with codes of 1, 4, 5, 12, 20, and 26 in Table 1 are included in this group. Basin depths reaching around 500 m are identified as deep, and samples with codes 10, 11, 14, 16, 22, 23, and 25 are also included in this group. Basins with a depth of more than 100 m are grouped as medium deep, and sample nos. 6, 8, 17, 21, 24, 28, 29, 30, and 31 are included in this group. Finally, basins with a thickness of less than 100 m were classified as shallow-depth basins, and samples 2, 3, 7, 9, 13, 15, 18, 19, and 27 were also included in this group (Table 1). The graphical variation of all the groups was examined together, and it was understood that the *a-coefficients* indeed varied within a certain range for certain depths. Nevertheless, the presence of some deviations can be interpreted in different ways. For example, Hinzen et al. (2004) have completed their work in the Lower Rhine region of Germany. However, a different correlation is encountered in the study conducted by Ibs-von Seht and Wohlenberg (1999) in the same area. This discrepancy is all about the average thickness of the basins. The sudden local deepening of the basins in certain regions does not make a significant

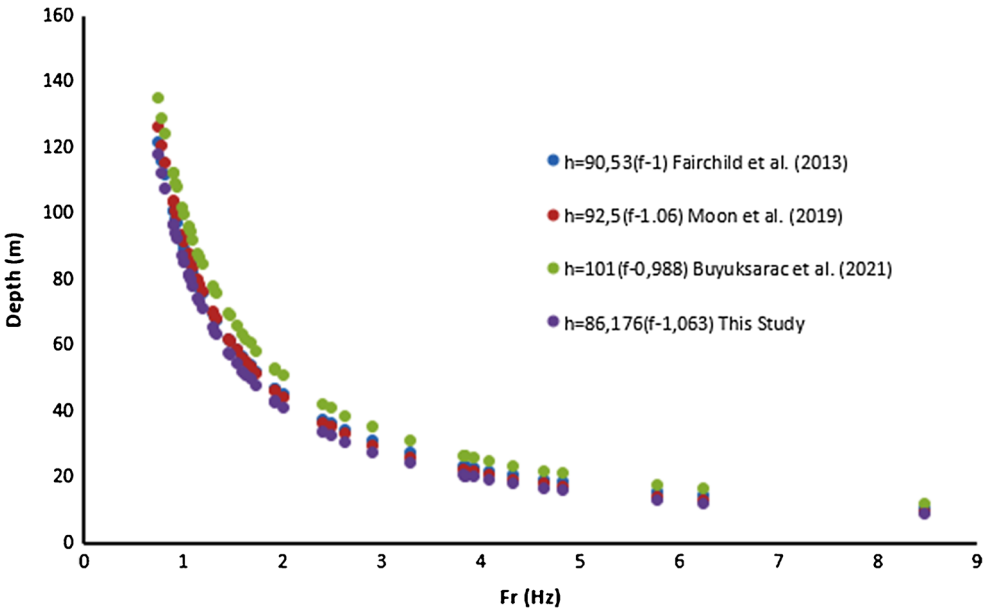

Fig. 9 Change of *fr-h* curves obtained in areas with soil characteristics as observed at Çanakkale Basin

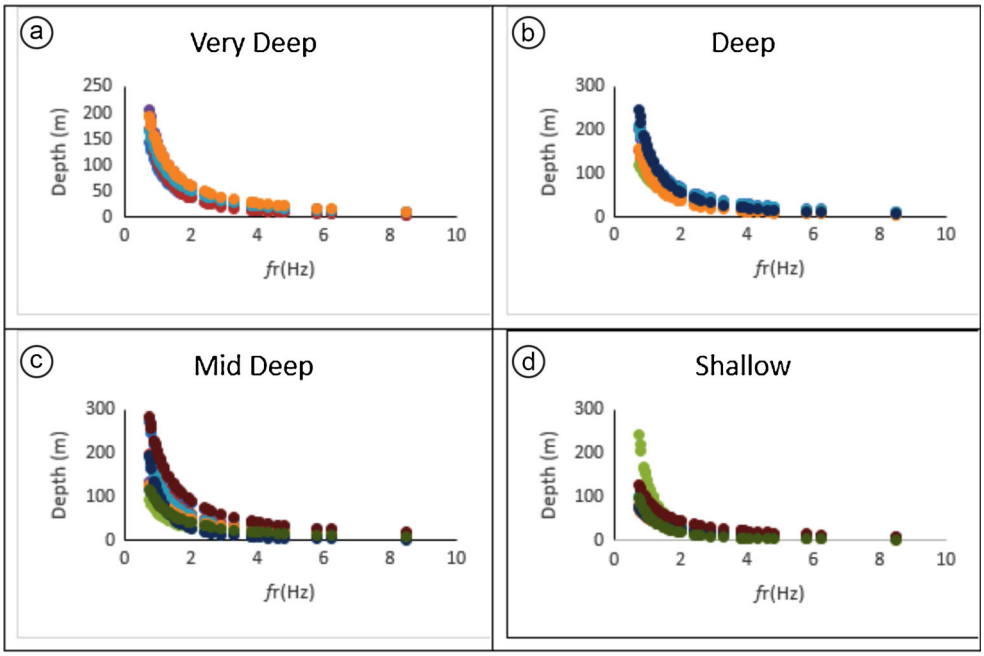

Fig. 10 Depth groupings created from 30 different equations. (**a**) Very deep, (**b**) deep, (**c**) medium deep, and (**d**) shallow areas

change in the average thickness of the basin, so the resonance frequency does not change. In this case, deviation values may occur in the regression analysis. The calculations of the depth groups, considering the resonance frequencies obtained for Çanakkale Basin, are given in Fig. 10. When four different graphic groups are examined, generally equivalent changes are observed. Low frequency deviations are noticeable at medium and shallow depths. In these curves and graphs created by using the resonance frequency values of Çanakkale Basin, a frequency value around 7 Hz was not observed. This situation is completely caused by the data used and does not indicate any special situation.

On the other hand, the *fr-h* curves obtained in 30 different studies given in Table 1 are shown in a single graphic in the resonance frequency range between 1 and 7 Hz (Fig. 11). A similar graph is found in Büyüksaraç et al. (2021) using

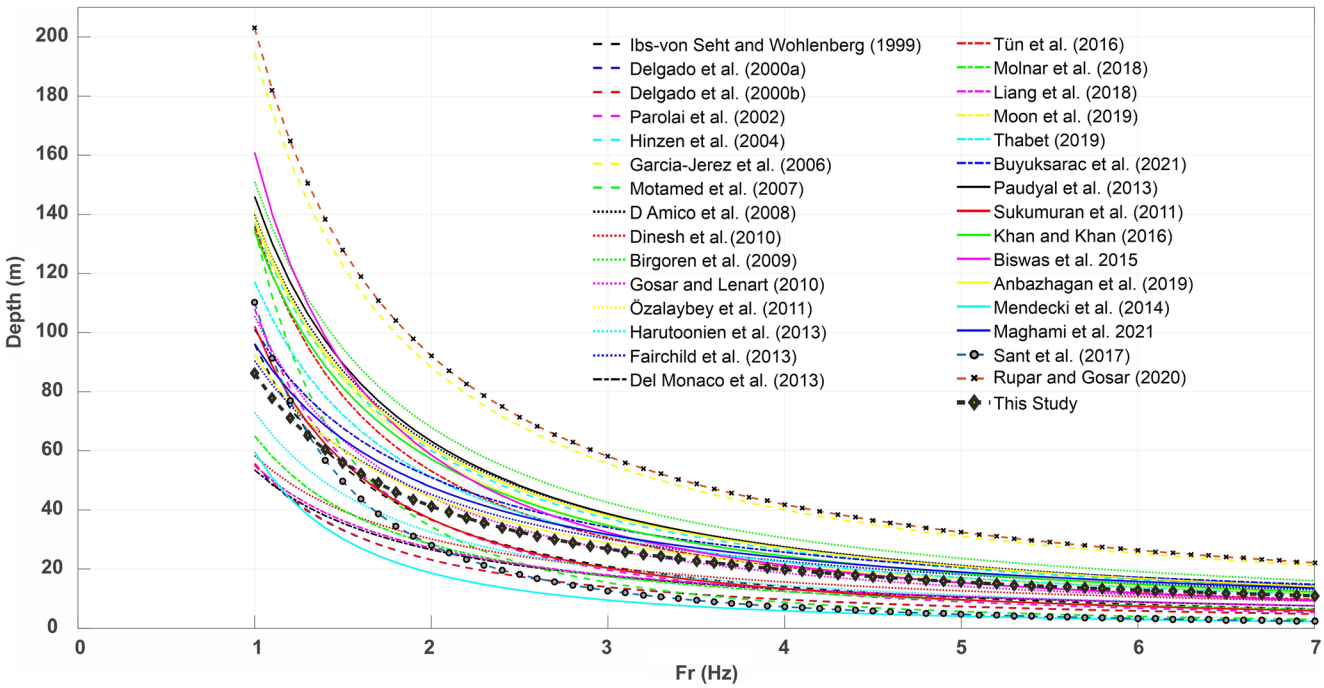

Fig. 11 Variation of bedrock depth with different formulas

Antakya resonance frequency values for 21 correlations for Antakya (Turkey) basin. In the figure, the abrupt changes of depth values at low frequency values can be shown as the remarkable common point of all studies. On the other hand, it is noteworthy that the curve obtained by Rupar and Gosar (2020) is distinctly different from the others. Of course, the field specific soil conditions have an important role in such studies. However, this excessive deviation should also have a valid explanation. Is this justification dependent on soil conditions or is it based on the data set used? It should be examined in detail.

Conclusions

Two different case studies were conducted within the scope of this study; the first case is to calculate the depth of the bedrock depending on the resonance frequency values obtained from the microtremor surveys previously performed in Çanakkale city. For this purpose, an exponential regression analysis, which has been successfully applied by different researchers, was performed. Fundamental mode Rayleigh wave ellipticity was obtained, and an empirical function was established for the whole basin by graphing variation in bedrock depth versus resonance frequency (Eq. 2). This exponential function provides an important approach to determine bedrock depth in Çanakkale central settlement and contributes to determine the basin character, which is another important aspect of this study. Accordingly, the obtained values have given the opportunity to be compared with the studies carried out in different parts of the world so far. The resonance frequency is the basic variable of the Eq. (1). However, these frequency values cannot be determined by any equation in determining the thickness of all weak sedimentary basins. The validity of Eq. (1) depends highly on the determination of the coefficients *a* and *b* that define the basin as characteristic at the regional scale. On the other hand, since the *b-coefficient* is an exponential value, it does not have a wide range of variation (Fig. 3). It is observed that the *b-coefficient* mostly varies between the values of 1 and 1.5. The value of *b-coefficients* greater than 1.5 is generally seen in shallow basins (Motamed et al. 2007; Sant et al. 2017). However, the *a-coefficient* can vary widely. This change is compatible with the depth structure of the basin. Accordingly, *a-coefficient* has big values in deep basins such as Cologne Area (Germany), Lower Rhine Embayment (Germany), Western Lower Rhine Embayment (Germany), Izmit Bay area (Turkey), Japan, and Indo-Gangetic Plain (India) in the range 96 and 234, averagely 138, whereas in shallow basins such as Segura river valley (South-eastern Spain), Bajo Segura Basin (South-eastern Spain), Bam Area (Iran), Bangalore City Deccan peninsular region (India), Western Sydney (Australia), Pearl River Delta (China), Singapore, Upper Silesian Coal Basin Sosnowiec, and Bytom and Chorzow (Poland), it has small values between 55 and 134, averagely 70.

Declarations

Conflict of interest The authors declare no competing interests.

References

Aki K (1965) Maximum likelihood estimate of b in the formula log N=a-bM and its confidence limits. Bull. Earthquake Res Inst., Tokyo Univ 43:237–239

Altınok Y, Alpar B, Yaltırak C, Pınar A, Özer, N (2012) The earthquakes and related tsunamis of October 6, 1944 and March 7, 1867; NE Aegean Sea. Natural Hazards 60:3–25

Ambraseys NN, Finkel CF (1995) The seismicity of Turkey and adjacent areas: a historical review, 1500–1800 edn. Eren Pub, Istanbul, p 240

Anbazhagan P, Janarthana Boobalan A, Shaivan HS (2019) Establishing empirical correlation between sediment thickness and resonant frequency using HVSR for the Indo-Gangetic Plain. Curr Sci 117(9): 1482–1491. https://doi.org/10.18520/cs/v117/i9/1482-1491

Atabey E, Ilgar A, Sakıtaş A (2004) Çanakkale Havzasinin Orta-Üst Miosen Stratigrafisi, 128th edn. MTA Dergisi, Çanakkale, pp 79–97

Bekler T, Demirci A (2018) Preliminary observations and assessment of Çanakkale-Ayvacık earthquake activity Çanakkale-Ayvacık Deprem Etkinliği İlksel Gözlemleri ve Değerlendirmeleri. Çanakkale Onsekiz Mart University. J Grad Sch Nat Appl Sci 4(1):1–13

Bekler T, Demirci A, Ekinci YL, Büyüksaraç A (2019) Analysis of local site conditions through geophysical parameters at a city under earthquake threat: Çanakkale, NW Turkey. J Appl Geophys 63:31–39. https://doi.org/10.1016/j.jappgeo.2019.02.009

Birgören G, Özel O, Siyahi B (2009) Bedrock depth mapping of the coast south of Istanbul: comparison of analytical and experimental analyses. Turk J Earth Sci 18:315–329. https://doi.org/10.3906/yer-0712-3

Biswas R, Baruah S, Bora DK (2015) Mapping sediment thickness in Shillong City of Northeast India through empirical relationship. J Earthquakes 2015:572619. https://doi.org/10.1155/2015/572619

Büyüksaraç A, Bektaş Ö, Över S, Kaçın S (2021) Investigation of the relationship between depth of bedrock and vulnerability in Antakya (South of Turkey) city center (*in review*).

D'Amico V, Picozzi M, Baliva F, Albarello D (2008) Ambient noise measurements for preliminary site-effects characterization in the urban area of Florence, Italy. Bull Seismol Soc Am 98(3):1373–1388. https://doi.org/10.1785/0120070231

Del Monaco F, Tallini M, De Rose C, Durante F (2013) HVNSR survey in historical downtown L'Aquila (central Italy): site resonance properties vs. subsoil model. Eng Geol 158:34–47. https://doi.org/10.1016/j.enggeo.2013.03.008

Delgado J, Casado CL, Estevez A, Giner J, Cuenca A, Molina S (2000a) Mapping soft soils in the Segura river valley (SE Spain): a case study of microtremors as an exploration tool. J Appl Geophys 45:19–32

Delgado J, Casado CL, Giner J, Estevez A, Cuenca A, Molina S (2000b) Microtremors as a geophysical exploration tool: applications and limitations. Pure Appl Geophys 157:1445–1462

Dinesh BV, Nair GJ, Prasad AGV, Nakkeeran PV, Radhakrishna MC (2010) Estimation of sedimentary layers shear wave velocity using micro-tremor H/V ratio measurements for Bangalore city. Soil Dyn Earthq Eng 30:1377–1382. https://doi.org/10.1016/j.soildyn.2010.06.012

Fäh D, Kind F, Lang K, Giardini D (2001) Earthquake scenarios for the city of Basel. Soil Dynamics and Earthquake Engineering 21(5): 405–413

Fairchild GM, Lane JW, Voytek EB, LeBlanc DR (2013) Bedrock topography of western Cape Cod, Massachusetts, based on bedrock altitudes from geologic borings and analysis of ambient seismic noise by the horizontal-to-vertical spectral-ratio method, U.S. Geological Survey Scientific Investigations Map 3233, 1 sheet, maps variously scaled, p 17. Pamphlet, on one CD–ROM. http://pubs.usgs.gov/sim/3233.Accessed 20 Feb 2017.

Field EH (1996) Spectral amplification in a sediment-filled valley exhibiting clear basin-edge-induced waves. Bull Seismol Soc Am 86:991–1005

Ganas A, Elias P, Kapetanidis V, Valkaniotis S, Briole P, Kassaras I, Argyrakis P, Barberopoulou A, Moshou A (2019) The July 20, 2017 M6.6 Kos earthquake: seismic and geodetic evidence for an active north-dipping normal fault at the western end of the Gulf of Gökova (SE Aegean Sea). Pure Appl Geophys 176:4177–4211. https://doi.org/10.1007/s00024-019-02154-y

García-Jerez A, Luzón F, Navarro M, Pérez-Ruiz A (2006) Characterization of the sedimentary cover of the Zafarraya basin, southern Spain, by means of ambient noise. Bull Seismol Soc Am 96(3):957–967. https://doi.org/10.1785/0120050061

Gorgun E, Albora AM (2017) Seismotectonic investigation of Biga Peninsula in SW Marmara region using steerable filter technique, potential field data and recent seismicity. Pure Appl Geophys 174: 3889–3904. https://doi.org/10.1007/s00024-017-1604-0

Gorgun E, Kalafat D, Kekovali K (2020) Source mechanisms and stress field of the 2017 Ayvacik/Canakkale earthquake sequence in NW Turkey. Ann Geophysics, 63. https://doi.org/10.4401/ag-8194

Gosar A, Lenart A (2010) Mapping the thickness of sediments in the Ljubljana Moor basin (Slovenia) using microtremors. Bull Earthq Eng 8:501–518. https://doi.org/10.1007/s10518-009-9115-8

Harutoonian P, Leo CJ, Tokeshi K, Doanh T, Castellaro S, Zou JJ, Liyanapathirana DS, Wong H (2013) Investigation of dynamically compacted ground by HVSR-based approach. Soil Dyn Earthq Eng 46:20–29. https://doi.org/10.1016/j.soildyn.2012.12.004

Hinzen KG, Weber B, Scherbaum F (2004) On the resolution of H/V measurements to determine sediment thickness, a case study across a normal fault in the Lower Rhine Embayment, Germany. J Earthq Eng 8(6):909–926. https://doi.org/10.1142/S136324690400178X

Ibs-von Seht M, Wohlenberg J (1999) Microtremors measurements used to map thickness of soft soil sediments. Bull Seismol Soc Am 89: 250–259

Kalafat D, Kekovalı K, Pınar A (2014) Source Characteristics of the January 8, 2013 (Mw=5.7) and May 24, 2014 (Mw=6.8) North Aegean Earthquakes and Their Aftershocks. İstanbul Earth Science Review 27(2):59–76

Khan S, Khan MA (2016) Mapping sediment thickness of the Islamabad City using empirical relationships: implications for seismic hazards assessment. J Earth Syst Sci 125(3):623–644

Konno K, Omachi T (1998) Ground-motion characteristics estimated from spectral ratio between horizontal and vertical components of microtremor. Bulletine of. Seismological. Soc Am 88:228–241

Kuo C, Chen C, Lin C, Wen K, Huang J, Chang SJ (2016) S-wave velocity structure and site effect parameters derived from microtremor arrays in the Western Plain of Taiwan. J Asian Earth Sci 128(1):27–41. https://doi.org/10.1016/j.jseaes.2016.07.012

Kürçer A, Chatzipetros A, Tutkun SZ, Pavlides S, Ateş Ö, Valkaniotis S (2008) The Yenice–Gönen active fault (NW Turkey): active tectonics and palaeoseismology. Tectonophysics 453(1–4):263–275. https://doi.org/10.1016/j.tecto.2007.07.010

Lermo J, Chavez-Garcia FJ (1994) Are microtremors useful in site response evaluation? Bull Seismol Soc Am 84:1350–1364

Liang D, Gan F, Zhang W, Jia L (2018) The application of HVSR method in detecting sediment thickness in karst collapse area of Pearl River Delta, China. Environ Earth Sci 77:259. https://doi.org/10.1007/s12665-018-7439-x

Ma J, Dong L, Zhao G, Li X (2018) Qualitative method and case study for ground vibration of tunnels induced by fault-slip in underground mine. Int J Rock Mech Min Sci 106(2018):213–222. https://doi.org/10.1016/j.ijrmms.2018.04.032

Ma J, Dong L, Zhao G, Li X (2019) Ground motions induced by mining seismic events with different focal mechanisms. Int J Rock Mech Min Sci 116(2019):99–110. https://doi.org/10.1016/j.ijrmms.2019.03.009

Maghami S, Sohrabi-Bidar A, Bignardi S, Zarean A, Kamalian M (2021) Extracting the shear wave velocity structure of deep alluviums of "Qom" Basin (Iran) employing HVSR inversion of microtremor recordings. J Appl Geophys 185:104246. https://doi.org/10.1016/j.jappgeo.2020.104246

Mendecki MJ, Bieta B, Mycka M (2014) Determination of the resonance frequency – thickness relation based on the ambient seismic noise records from Upper Silesia Coal Basin. Contemp Trends Geosci 3: 41–51. https://doi.org/10.2478/ctg-2014-0021

Molnar S, Cassidy JF, Castellaro S, Cornou C, Crow H, Hunter JA, Matsushima S, Sánchez-Sesma FJ, Yong A (2018) Application of microtremor horizontal-to-vertical spectral ratio (MHVSR) analysis for site characterization: state of the art. Surv Geophys 39:613–631. https://doi.org/10.1007/s10712-018-9464-4

Moon SW, Subramaniam P, Zhang Y, Vinoth G, Ku T (2019) Bedrock depth evaluation using microtremor measurement: empirical guidelines at weathered granite formation in Singapore. J Appl Geophys 171:103866

Motamed R, Ghalandarzadeh A, Tawhata I, Tabatabaei SH (2007) Seismic microzonation and damage assessment of Bam city, southeastern Iran. J Earthq Eng 11(1):110–132. https://doi.org/10.1080/13632460601123164

Nakamura Y (1989) A method for dynamic characteristics estimations of subsurface using microtremors on the ground surface. Q Rep RTRI Jpn 30:25–33

Nakamura Y (2008) On the H/V spectrum. The 14th World Conference on Earthquake Engineering, Beijing

Özalaybey S, Zor E, Ergintav S, Tapırdamaz MC (2011) Investigation of 3-D basin structures in the Izmit Bay area (Turkey) by single-station microtremor and gravimetric methods. Geophys J Int 186:883–894. https://doi.org/10.1111/j.1365-246X.2011.05085.x

Özden S, Över S, Poyraz SA, Güneş Y, Pınar A (2018) Tectonic implications of the 2017 Ayvacik (Canakkale) earthquakes, Biga Peninsula, NW Turkey. J Asian Earth Sci 154:125–141

Parolai S, Bormann P, Milkereit C (2002) New relationships between Vs, thickness of sediments, and resonance frequency calculated by the H/V ratio of seismic noise for Cologne Area (Germany). Bull Seismol Soc Am 92:2521–2527

Paudyal YR, Yatabe R, Bhandary NP, Dahal RK (2013) Basement topography of the Kathmandu Basin using microtremor observation. J Asian Earth Sci 62:627–637. https://doi.org/10.1016/j.jseaes.2012.11.011

Rupar L, Gosar A (2020) Mapping the thickness of Quaternary sediments in the Iška alluvial fan (central Slovenia) usıng microtremor method. Acta Geodyn Geomater 17(2 (198)):177–190. https://doi.org/10.13168/AGG.2020.0013

Sant DA, Parvez IA, Rangarajan G, Patel SJ, Bhatt MN, Salam TAS (2017) Subsurface profiling along Banni Plains and bounding faults,

Kachchh, Western India using microtremors method. J Asian Earth Sci 146:326–336. https://doi.org/10.1016/j.jseaes.2017.06.002

Sukumaran P, Parvez IA, Sant DA, Rangarajan G, Krishnan K (2011) Profiling of late Tertiary–early Quaternary surface in the lower reaches of Narmada valley using microtremors. J Asian Earth Sci 41:325–334

Thabet M (2019) Site-specific relationships between bedrock depth and HVSR fundamental resonance frequency using KiK-NET data from Japan. Pure Appl Geophys 176:4809–4831. https://doi.org/10.1007/s00024-019-02256-7

Tün M, Pekkan E, Ozel O, Guney Y (2016) An investigation into the bedrock depth in the Eskisehir Quaternary Basin (Turkey) using the microtremor method. Geophys J Int 207(1):589–607. https://doi.org/10.1093/gji/ggw294

Tunusluoğlu MC, Karaca Ö (2018) Liquefaction severity mapping based on SPT data: a case study in Canakkale city (NW Turkey). Environ Earth Sci 77(12)

Wathelet M, Chatelain JL, Cornou C, Di Giulio G, Guillier B, Ohrnberger M, Savvaidis A (2020) Geopsy: a user-friendly open-source tool set for ambient vibration processing. Seismol Res Lett 91(3):1878–1889. https://doi.org/10.1785/0220190360

Yamanaka H, Takemura M, Ishida H, Niwa M (1994) Characteristics of long-period microtremors and their applicability in exploration of deep sedimentary layers. Bull Seismol Soc Am 84(6):1831–1841

Yiğitbaş E (2015) Jeolojik–Antropojenik Sebep–Sonuç İlişkileri Açısından Çanakkale Heyelanlarına Toplu Bakış. Çanakkale Heyelanları Kitabı, Altın Kalem Yayınları ISBN 978-605-9837-26-2